2013 European Control Conference (ECC)
July 17-19, 2013, Zürich, Switzerland.

On a reduced-order two-track car model including longitudinal and lateral load transfer

Alessandro Rucco, Giuseppe Notarstefano and John Hauser

Abstract— **In this paper we propose a novel reduced-order car model that captures some key features for aggressive maneuvering of complex car vehicles. The proposed model, called *RigidCar*, consists of a rigid body interacting with the ground at four contact points (two-track car) and including tire models and load transfer. The model does not include suspension models, thus keeping a reasonable level of complexity. Load transfer (both longitudinal and lateral) is taken into account by explicitly imposing the holonomic constraints and computing the reaction forces of the ground at the four contact points. Since the vehicle interacts with the ground at four contact points, it results to be a *hyper-static* structure so that reaction forces are not uniquely determined. We use the *Principle of Least Work* to get a compatibility equation and thus resolving the indeterminateness. We provide numerical computations validating the proposed model with respect to a multi-body virtual prototype on an aggressive ISO lane-change maneuver.**

I. Introduction

In order to explore the dynamic capabilities of real vehicles, several software tools have been developed, thus helping engineers to understand the behavior of real vehicles [1], [2]. The basic idea is to build a *virtual prototype* that allows to perform important dynamic analyses of the vehicle before the construction of a real prototype.

Many models have been introduced in the literature to capture the main behavior of a car vehicle [3], [4], [5]. The *two-track* model is a planar rigid model that approximates the vehicle as a rigid body with four wheels. Several versions of this model are available in the literature with many different levels of complexity [6], [7], [8], [9]. Suspension systems play an important role in vehicle handling behavior by distributing the load on the ground, and reducing vibrations due to the contact of wheels with the ground even with an uneven road profile. In this paper we do not model the suspension system, and therefore we refer the reader to [10] for an overview of the different type of suspensions. Indeed, our main goal is to build a simplified model reproducing the main dynamic features of the real vehicle, as well as the longitudinal and lateral load transfer, without explicitly modeling the suspensions. The load transfer has an important influence on the vehicle behavior. For example, it influences the minimum lap-time trajectory, [11]. For this reason, it is essential to understand the influence of the force distribution. Due to the highly nonlinear distribution of vehicle forces on the ground, the studies in this field have focused on the development and analysis of models with increasingly sophisticated suspension, see, e.g., [8]. On the other hand, developing a simple model that still is able to take into account this phenomenon is of key interest. Indeed, such a model can be used in the design of handling analysis and control toolboxes for complex vehicle models.

The contributions of the paper are as follows. First, we develop reduced-order model for a two-track car vehicle, which includes tire models and load transfer (both longitudinal and lateral). The model does not include suspension models, thus keeping a reasonable level of complexity. Load transfer (both longitudinal and lateral) is taken into account by explicitly imposing the holonomic constraints and computing the reaction forces of the ground at the four contact points. Since the vehicle interacts with the ground at four contact points, it results to be a *hyper-static* structure so that reaction forces are not uniquely determined. We use the *Principle of Least Work* to get a compatibility equation and thus resolving the indeterminateness.

Second, we validate the proposed car model. We proceed as follows. We let a multi-body software generate a trajectory for a complex car model. Such trajectory is used as desired curve for an unconstrained L_2 minimization problem. By using a trajectory exploration strategy, based on nonlinear optimal control techniques and continuation strategy, we compute an optimal RigidCar trajectory. The numerical computations confirm that RigidCar model captures the main dynamic features of the full-vehicle as, in particular, the longitudinal and lateral load transfer, even thought the RigidCar has not a suspension model.

The rest of the paper is organized as follows. In Section II we introduce and develop the RigidCar model. In Section III we provide numerical computations validating the RigidCar model with respect to a highly complex multi-body model on an aggressive trajectory.

II. Rigid Car model development

In this section we derive the car model (RigidCar) proposed in the paper. The car model consists of a single rigid body that interacts with the road at four body-fixed contact points according to a suitable tire model.

The vehicle is geometrically symmetric about the longitudinal axis, i.e. the center of mass is located at distance d from the lateral contact points. We denote a and b the distances of the center of mass from the front and rear contact points, so that $\ell = a + b$ is the wheelbase.

Alessandro Rucco and Giuseppe Notarstefano are with the Department of Engineering, Università del Salento (University of Lecce), Via per Monteroni, 73100 Lecce, Italy, {alessandro.rucco, giuseppe.notarstefano}@unisalento.it

John Hauser is with the Department of Electrical and Computer Engineering, University of Colorado, Boulder, CO 80309-0425, USA, hauser@colorado.edu

A planar view of the rigid car model is shown in Figure 1. In Table I we provide a list of the car symbols used in the paper. A rigorous definition of these symbols will be given in the following model development.

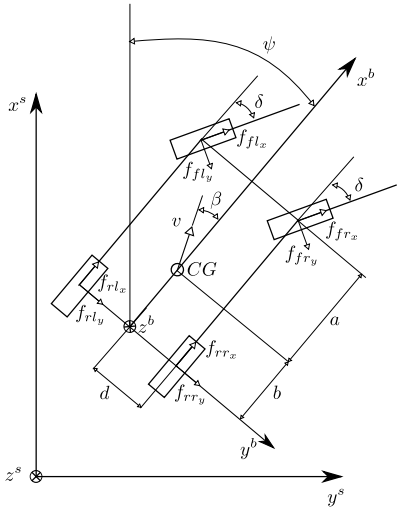

Fig. 1: RigidCar model. The figure shows the quantities used to describe the model.

b	distance between rear axle and CG	m
a	distance between front axle and CG	m
ℓ	wheelbase, $\ell = (a + b)$	m
d	distance between lateral axle and CG	m
m	vehicle's mass	kg
h	height of the centre of mass from the ground	m
c	suspension stiffness coefficient	Nodim
I_{zz}, I_{xz}	inertia's terms (wrt z-axis and x-z plane)	kg m^2
μ_x, μ_y	longitudinal, lateral force coefficients	Nodim
β	side slip angle	rad
g	gravity acceleration	m/s^2
f_x, f_y, f_z	longitudinal, lateral, normal, tire force	N
x, y	longitudinal, lateral position midpoint rear axle	m
ψ	car yaw angle	rad
v_x, v_y	longitudinal, lateral velocity CG	m/s
r	car yaw rate	rad/s
δ	front wheel steer angle	rad
κ	longitudinal slip	Nodim

TABLE I: Nomenclature

The first idea at the basis of our RigidCar model is the following. We start from the (unconstrained) six-degree of freedom rigid body model and then impose the four contact point constraints in order to have an explicit expression for the reaction forces.

The body-frame of the car is located at the midpoint of the rear (contact points) axle with x-y-z axes oriented in a forward-right-down fashion. We let $\mathbf{x} = [x\ y\ z]^T \in \mathbb{R}^3$ and $R \in SO(3)$ denote the position and orientation of the frame with respect to a fixed spatial-frame with x-y-z axes oriented in a north-east-down fashion. R maps vectors in the body frame to vectors in the spatial frame so that, for instance, the spatial angular velocity ω^s and the body angular velocity ω^b are related by $\omega^s = R\omega^b$ and $\omega^b = R^T\omega^s$. Similarly, $\mathbf{x}^s = \mathbf{x} + R\,\mathbf{x}^b$ gives the spatial coordinates of a point on the body with body coordinates $\mathbf{x}^b \in \mathbb{R}^3$.

The orientation R of the (unconstrained) rigid car model can be parameterized (using Roll-Pitch-Yaw parametrization) as follows

$$R = R(\psi,\theta,\varphi) = R_z(\psi)R_y(\theta)R_x(\varphi) = \\ = \begin{bmatrix} c_\psi c_\theta & c_\psi s_\theta s_\varphi - s_\psi c_\varphi & c_\psi s_\theta c_\varphi + s_\psi s_\varphi \\ s_\psi c_\theta & s_\psi s_\theta s_\varphi + c_\psi c_\varphi & s_\psi s_\theta c_\varphi - c_\psi s_\varphi \\ -s_\theta & c_\theta s_\varphi & c_\theta c_\varphi \end{bmatrix},$$

where φ, θ and ψ are respectively the roll, pitch and yaw angles (we use the notation $c_\psi = \cos(\psi)$, etc.). In the rest of the paper, for brevity, we use the notation $\phi = [\psi, \varphi, \theta]^T$. The vector

$$q = [x, y, \psi, z, \varphi, \theta]^T = [q_r, q_c]^T$$

provides a valid set of generalized coordinates for dynamics calculations. The coordinates $q_r = [x, y, \psi]^T$ are the *reduced* unconstrained car coordinates, while $q_c = [z, \varphi, \theta]^T$ are the *constrained* coordinates.

A. Tire models

Tires are one of the key components of the vehicle and have an important impact on the performance. To capture the complex behavior of the tires several models have been developed in the literature [6], [12], [13]. We introduce a general tire model, whose specific expression can be one of those available in the literature. In particular, in the numerical computations provided in the paper a suitable Pacejka's model is used (see [14] for more details). We begin by providing some notation. We associate two indices, $i \in \{f, r\}$ (front/rear) and $j \in \{r, l\}$ (right/left), to each tire quantity when we want to provide an expression holding for a generic tire. Thus, for example, we denote the generic normal tire force f_{ij_z}, meaning that we are referring to f_{fr_z} (f_{fl_z}) for the front right (left) tires and f_{rr_z} (f_{rl_z}) for the rear right (left) ones.

The forces tangent to the road plane, f_{ij_x} and f_{ij_y}, depend on the normal tire force and on the longitudinal and lateral tire slips. The longitudinal slip κ_{ij} is the normalized difference between the angular velocity of the driven wheel ω_{ij_w} and the angular velocity of the free-rolling $\omega_{ij_0} = v_{ij_{cx}}/r_{ij_w}$, with $v_{ij_{cx}}$ the contact point longitudinal velocity and r_{ij_w} the effective rolling radius of the tire,

$$\kappa_{ij} = \frac{\omega_{ij_w} - \omega_{ij_0}}{\omega_{ij_0}} = -\frac{v_{ij_{cx}} - r_{ij_w}\omega_{ij_w}}{v_{ij_{cx}}}.$$

The lateral slip (or side-slip) β_{ij} is defined as $\tan\beta_{ij} = v_{ij_{cy}}/v_{ij_{cx}}$, with $v_{ij_{cy}}$ the lateral velocity.

Assumption 2.1: The forces tangent to the road plane, f_{ij_x} and f_{ij_y}, depend linearly on the normal forces f_{ij_z}, that is

$$f_{ij_x} = -f_{ij_z}\mu_{ij_x}(\kappa_{ij}, \beta_{ij}),$$
$$f_{ij_y} = -f_{ij_z}\mu_{ij_y}(\kappa_{ij}, \beta_{ij}),$$

where μ_{ij_x} and μ_{ij_y} are the combined longitudinal and lateral force coefficients, respectively. □

The front forces expressed in the body frame, $f^b_{fj_x}$ and $f^b_{fj_y}$, are obtained by rotating the forces in the tire frame according to the steering angle δ, so that, e.g., $f^b_{fj_x} = f_{fj_x}c_\delta - f_{fj_y}s_\delta$. Substituting the above expressions for f_{fx} and f_{fy}, we get

$$\begin{aligned} f^b_{fj_x} &= -f_{fj_z}\big(\mu_{fj_x}(\kappa_{fj},\beta_{fj})c_\delta - \mu_{fj_y}(\kappa_{fj},\beta_{fj})s_\delta\big) \\ &:= -f_{fj_z}\tilde{\mu}_{fj_x}(\kappa_{fj},\beta_{fj},\delta). \end{aligned}$$

In the rest of the paper, abusing notation, we will suppress the 'tilde' and use $\mu_{fj_x}(\kappa_{fj},\beta_{fj},\delta)$ to denote $\tilde{\mu}_{fj_x}(\kappa_{fj},\beta_{fj},\delta)$.

We assume to control the longitudinal slips κ_{ij}. Thus, the *control inputs* of the car turn to be:

- κ_{ij}, the front/rear, right/left longitudinal slips,
- δ, the front wheel steering angle.

B. Constrained Lagrangian dynamics

Next, we develop the constrained planar model of the rigid car that allows to include the load transfer. To describe the motion in the plane, we derive the equations of motion of the unconstrained system and explicitly incorporate the constraints (rather than choosing a subset of generalized coordinates). This allows us to have an explicit expression for the normal (constraint) forces. The derivation follows the idea developed for a single-track car with longitudinal load transfer, see [15], [14].

We derive the dynamics of the unconstrained system via the Euler-Lagrange equations. To do this, we define the Lagrangian $\mathcal{L}$ as the difference between the kinetic and potential energies $\mathcal{L}(q,\dot{q}) = T(q,\dot{q}) - V(q)$. The equations of motion for the unconstrained system are given by the Euler-Lagrange equations

$$\frac{d}{dt}\frac{\partial \mathcal{L}}{\partial \dot{q}}^T - \frac{\partial \mathcal{L}}{\partial q}^T = U$$

where U is the set of generalized forces. Exploiting the Euler-Lagrange equations, we get

$$M(q)\ddot{q} + C(q,\dot{q}) + G(q) = U \tag{1}$$

with $M(q)$, $C(q,\dot{q})$ and $G(q)$ respectively the mass matrix, and the Coriolis and gravity vectors.

The longitudinal and lateral forces arising from the tire-road interactions at the front and rear contact points, $f = [f_{fr_x}, f_{fr_y}, f_{fl_x}, f_{fl_y}, f_{rr_x}, f_{rr_y}, f_{rl_x}, f_{rl_y}]^T$, are converted into the generalized forces U by using the *principle of virtual work*, $< f, v^b_{cp} >=< U, \dot{q} >$, where $v^b_{cp} = [v^b_{fr_x}, v^b_{fr_y}, v^b_{fl_x}, v^b_{fl_y}, v^b_{rr_x}, v^b_{rr_y}, v^b_{rl_x}, v^b_{rl_y}]^T$ are the longitudinal and lateral velocities at the front and rear contact points. Computing the Jacobian matrix $J_f(\phi)$ mapping $\dot{q}$ to the front and rear contact point velocities expressed in the body frame, $v^b_{cp} = J_f(\phi)\dot{q}$, we get $< J_f(\phi)^T f, \dot{q} >=< U, \dot{q} >$, so that

$$U = J_f^T(\phi) f.$$

The front and rear, left and right, contact points coordinates expressed in the body frame are $\mathbf{x}^b_{fr} = [\ell, d, 0]^T$, $\mathbf{x}^b_{fl} = [\ell, -d, 0]^T$, $\mathbf{x}^b_{rr} = [0, d, 0]^T$ and $\mathbf{x}^b_{rl} = [0, -d, 0]^T$. The coordinates in the spatial frame, respectively $\mathbf{x}^s_{ij} = [x^s_{ij}, y^s_{ij}, z^s_{ij}]^T$, are $\mathbf{x}^s_{ij} = \mathbf{x} + R\,\mathbf{x}^b_{ij}$, so that the velocities in the spatial frame are

$$v^s_{ij} = \dot{\mathbf{x}} + R\,\omega^b \times \mathbf{x}^b_{ij} = \dot{\mathbf{x}} - R\,\mathbf{x}^b_{ij} \times \omega^b = \dot{\mathbf{x}} - R\,\hat{\mathbf{x}}^b_{ij} J_{\omega^b}(\phi)\dot{\phi},$$

where $\hat{\mathbf{x}}^b_{ij}$ is the skew-symmetric matrix associated to the vector $\mathbf{x}^b_{ij}$, while the velocities expressed in the body frame are

$$v^b_{ij} = R^T\dot{\mathbf{x}} - \hat{\mathbf{x}}^b_{ij} J_{\omega^b}(\phi)\dot{\phi} = J_{v^b_{ij}}(\phi)\dot{q}\,.$$

Thus, the Jacobian mapping the generalized velocities to the four contact points velocities, $J_f(\phi) = [J_{v^b_{fr_x}}, J_{v^b_{fr_y}}, J_{v^b_{fl_x}}, J_{v^b_{fl_y}}, J_{v^b_{rr_x}}, J_{v^b_{rr_y}}, J_{v^b_{rl_x}}, J_{v^b_{rl_y}}]^T$, turns to be

$$J_f(\phi) = \left[\ J_{f_1}(\phi)\ \middle|\ J_{f_2}(\phi)\ \right] =$$

$$\left[\begin{array}{ccc|ccc} c_\psi c_\theta & s_\psi c_\theta & -dc_\theta c_\varphi & -s_\theta & 0 & ds_\varphi \\ c_\psi s_\theta s_\varphi - s_\psi c_\varphi & s_\psi s_\theta s_\varphi + c_\psi c_\varphi & \ell c_\theta c_\varphi & c_\theta s_\varphi & 0 & -\ell s_\varphi \\ c_\psi c_\theta & s_\psi c_\theta & dc_\theta c_\varphi & -s_\theta & 0 & -ds_\varphi \\ c_\psi s_\theta s_\varphi - s_\psi c_\varphi & s_\psi s_\theta s_\varphi + c_\psi c_\varphi & \ell c_\theta c_\varphi & c_\theta s_\varphi & 0 & -\ell s_\varphi \\ c_\psi c_\theta & s_\psi c_\theta & -dc_\theta c_\varphi & -s_\theta & 0 & ds_\varphi \\ c_\psi s_\theta s_\varphi - s_\psi c_\varphi & s_\psi s_\theta s_\varphi + c_\psi c_\varphi & 0 & c_\theta s_\varphi & 0 & 0 \\ c_\theta c_\varphi & s_\psi c_\theta & dc_\theta c_\varphi & -s_\theta & 0 & -ds_\varphi \\ c_\psi s_\theta s_\varphi - s_\psi c_\varphi & s_\psi s_\theta s_\varphi + c_\psi c_\varphi & 0 & c_\theta s_\varphi & 0 & 0 \end{array}\right].$$

Next, we constrain the contact points to the road plane in order to compute the normal tire forces as the reaction forces with opposite sign. We impose the constraint that the contact points have zero velocity along the z axis. The velocity constraints are given by

$$\dot{z}_{ij} = e_3^T(R^T\dot{\mathbf{x}} - \hat{\mathbf{x}}^b_{ij} J_{\omega^b}(\phi)\dot{\phi}) = J_{v^b_{ij_z}}(\phi)\dot{q} = 0,$$

where $e_3 = [0,0,1]^T$, and z_{ij} is the vertical position of the contact point ij expressed in the body frame. The constraints may be written in the form $A(q)\dot{q} = 0$, where

$$\begin{aligned} A(q) &= \begin{bmatrix} J_{v^b_{fr_z}}(\phi) & J_{v^b_{fl_z}}(\phi) & J_{v^b_{rr_z}}(\phi) & J_{v^b_{rl_z}}(\phi) \end{bmatrix}^T \\ &= \left[\ A_1(\phi)\ \middle|\ A_2(\phi)\ \right] = \end{aligned}$$

$$\left[\begin{array}{ccc|ccc} c_\psi s_\theta c_\varphi + s_\psi s_\varphi & s_\psi s_\theta c_\varphi - c_\psi s_\varphi & -ds_\theta - \ell c_\theta s_\varphi & c_\theta c_\varphi & d & -\ell c_\varphi \\ c_\psi s_\theta c_\varphi + s_\psi s_\varphi & s_\psi s_\theta c_\varphi - c_\psi s_\varphi & ds_\theta - \ell c_\theta s_\varphi & c_\theta c_\varphi & -d & -\ell c_\varphi \\ c_\psi s_\theta c_\varphi + s_\psi s_\varphi & s_\psi s_\theta c_\varphi - c_\psi s_\varphi & -ds_\theta & c_\theta c_\varphi & d & 0 \\ c_\psi s_\theta c_\varphi + s_\psi s_\varphi & s_\psi s_\theta c_\varphi - c_\psi s_\varphi & ds_\theta & c_\theta c_\varphi & -d & 0 \end{array}\right]. \tag{2}$$

From the principle of virtual work, we get the vector of constraint generalized forces, U_c, in terms of normal contact-point forces, $\lambda = [-f_{fr_z} - f_{fl_z} - f_{rr_z} - f_{rl_z}]^T \in \mathbb{R}^4$ as

$$U_c = -A^T(q)\lambda.$$

Moreover, for the Assumption 2.1, the forces f depend linearly on the reaction forces, that is $f = F(\mu_{ij})\lambda$, for a suitable $F(\mu_{ij})$. Then we can rewrite the generalized forces, U, in terms of reaction forces, that is $U = J_f^T(q)F(\mu_{ij})\lambda$.

Hence the constrained equations of motion can be written as

$$\begin{aligned} M(q)\ddot{q} + C(q,\dot{q}) + G(q) &= J_f^T(q)F(\mu_{ij})\lambda - A^T(q)\lambda \\ A(q)\ddot{q} + \dot{A}(q)\dot{q} &= 0, \end{aligned}$$

where M, C, G and A are the one introduced in (1) and (2).

Enforcing the constraints $q_c(t) = \dot{q}_c(t) = \ddot{q}_c(t) = 0$, $\forall t \in \mathbb{R}$, the second equation becomes an identity, while the first equations becomes

$$\begin{bmatrix} M_{11}(q_r) & M_{12}(q_r) \\ M_{21}(q_r) & M_{22}(q_r) \end{bmatrix}\begin{bmatrix} \ddot{q}_r \\ 0 \end{bmatrix} + \begin{bmatrix} J_{f_1}^T(q_r)F(\mu_{ij}) \\ 0 \end{bmatrix}\lambda + \begin{bmatrix} 0 \\ A_2^T \end{bmatrix}\lambda + \begin{bmatrix} C_1(q_r,\dot{q}_r) \\ C_2(q_r,\dot{q}_r) \end{bmatrix} + \begin{bmatrix} G_1(q_r) \\ G_2(q_r) \end{bmatrix} = \begin{bmatrix} 0 \\ 0 \end{bmatrix},$$

so that we can rewrite the dynamics of the constrained system in terms of the unconstrained coordinates $q_r = [x, y, \psi]^T$ and the reaction forces λ as

$$\begin{bmatrix} M_{11}(q_r) & J_{f_1}^T(q_r)F(\mu_{ij}) \\ M_{21}(q_r) & A_2^T \end{bmatrix}\begin{bmatrix} \ddot{q}_r \\ \lambda \end{bmatrix} + \begin{bmatrix} C_1(q_r,\dot{q}_r) \\ C_2(q_r,\dot{q}_r) \end{bmatrix} + \begin{bmatrix} G_1(q_r) \\ G_2(q_r) \end{bmatrix} = \begin{bmatrix} 0 \\ 0 \end{bmatrix}. \tag{3}$$

where

$$M_{11}(q_r) = \begin{bmatrix} m & 0 & -mbs_\psi \\ 0 & m & mbc_\psi \\ -mbs_\psi & mbc_\psi & I_{zz} + mb^2 \end{bmatrix},$$

$$M_{21}(q_r) = \begin{bmatrix} 0 & 0 & 0 \\ -mhs_\psi & mhc_\psi & I_{xz} + mbh \\ -mhc_\psi & -mhs_\psi & 0 \end{bmatrix},$$

$$C_1(q_r,\dot{q}_r) = \begin{bmatrix} -mbc_\psi\dot{\psi}^2 \\ -mbs_\psi\dot{\psi}^2 \\ 0 \end{bmatrix}, C_2(q_r,\dot{q}_r) = \begin{bmatrix} 0 \\ 0 \\ (I_{xz} + mhb)\dot{\psi}^2 \end{bmatrix},$$

$$G_1(q_r) = \begin{bmatrix} 0 \\ 0 \\ 0 \end{bmatrix}, G_2(q_r) = \begin{bmatrix} -mg \\ 0 \\ mgb \end{bmatrix}.$$

Since the dynamics does not depend on the positions x and y, and the orientation ψ, we can work directly with the longitudinal velocity v_x, the lateral velocity v_y, and the yaw rate $r := \dot{\psi}$. To do this, note that, defining $q_v = [v_x, v_y, r]^T$,

$$\dot{q}_r = R_z(\psi)q_v \;\text{ and }\; \ddot{q}_r = R_z(\psi)\begin{bmatrix} \dot{v}_x - v_y r \\ \dot{v}_y + v_x r \\ \dot{r} \end{bmatrix}.$$

Expressing the dynamics in the body frame, equation (3) becomes

$$\begin{bmatrix} \mathcal{M}_{11} & \mathcal{M}_{12}(\mu_{ij}) \\ \mathcal{M}_{21} & \mathcal{M}_{22} \end{bmatrix}\begin{bmatrix} \dot{q}_v \\ \lambda \end{bmatrix} + \begin{bmatrix} \mathcal{C}_1(q_v) \\ \mathcal{C}_2(q_v) \end{bmatrix} + \begin{bmatrix} \mathcal{G}_1 \\ \mathcal{G}_2 \end{bmatrix} = \begin{bmatrix} 0 \\ 0 \end{bmatrix}, \tag{4}$$

where

$$\mathcal{M}_{11} = \begin{bmatrix} m & 0 & 0 \\ 0 & m & mb \\ 0 & mb & I_{zz} + mb^2 \end{bmatrix},$$

$$\mathcal{M}_{12} = \begin{bmatrix} -\mu_{fr_x} & -\mu_{fl_x} & -\mu_{rr_x} & -\mu_{rl_x} \\ -\mu_{fr_y} & -\mu_{fl_y} & -\mu_{rr_y} & -\mu_{rl_y} \\ d\mu_{fr_x} - \ell\mu_{fr_y} & -\ell\mu_{fl_y} - d\mu_{fl_x} & d\mu_{rr_x} & -d\mu_{rl_x} \end{bmatrix},$$

$$\mathcal{M}_{21} = \begin{bmatrix} 0 & 0 & 0 \\ 0 & mh & I_{xz} + mbh \\ -mh & 0 & 0 \end{bmatrix}, \mathcal{M}_{22} = \begin{bmatrix} 1 & 1 & 1 & 1 \\ d & -d & d & -d \\ -\ell & -\ell & 0 & 0 \end{bmatrix},$$

$$\mathcal{C}_1(q_v) = \begin{bmatrix} -mv_y r - mbr^2 \\ mv_x r \\ mbv_x r \end{bmatrix}, \mathcal{C}_2(q_v) = \begin{bmatrix} 0 \\ mhv_x r \\ mhv_y r + (I_{xz} + mhb)r^2 \end{bmatrix},$$

$$\mathcal{G}_1 = \begin{bmatrix} 0 \\ 0 \\ 0 \end{bmatrix}, \mathcal{G}_2 = \begin{bmatrix} -mg \\ 0 \\ mgb \end{bmatrix}.$$

The expression of the reaction forces, λ, cannot be univocally obtained by equation (4), since $\mathcal{M}_{22} \in \mathbb{R}^{3\times 4}$. This is due to the *hyper-static* nature of the contact point constraints. Next, we show how to develop a model that depends on a set of parameters related to the suspensions, but keeps the same level of complexity. In order to develop such a model we apply the Principle of Least Work to recover the reaction forces in a hyper-static structure (see [16] for more details).

We proceed as follows. We assume that the contact between the four contact points and the ground happens according to a strain model, as shown in Figure 2, and assume that the car structure is rigid. Then, we compute the total strain energy of the car due to the reaction forces at the four contact points, and minimize this energy.

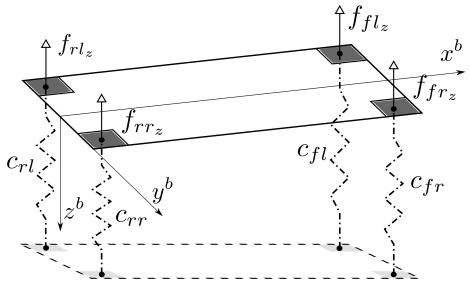

Fig. 2: Representation of the normal forces acting on the RigidCar model.

To do that, we derive explicitly three reaction forces as function of a fourth unknown. We choose f_{rl_z} as unknown. From equation (4), we have

$$\begin{bmatrix} f_{fr_z} \\ f_{fl_z} \\ f_{rr_z} \end{bmatrix} = -\begin{bmatrix} 1 & 1 & 1 \\ d & -d & d \\ -\ell & -\ell & 0 \end{bmatrix}^{-1} \left(\mathcal{M}_{21}\dot{q}_v + \mathcal{C}_2 + \mathcal{G}_2 - \begin{bmatrix} 1 \\ -d \\ 0 \end{bmatrix} f_{rl_z} \right).$$

Then, the total strain energy is given by

$$E = \sum_{\substack{i\in\{f,r\} \\ j\in\{r,l\}}} \frac{1}{2} c_{ij} f_{ij_z}^2 ,$$

where c_{ij} are coefficients that include material properties such as the Young's modulus. Therefore, for the Principle of Least Work, the reaction force f_{rl_z} is the one that minimize the strain energy:

$$\frac{\partial E(f_{rl_z})}{\partial f_{rl_z}} = \sum_{\substack{i\in\{f,r\} \\ j\in\{r,l\}}} c_{ij} f_{ij_z} \frac{\partial f_{ij_z}(f_{rl_z})}{\partial f_{rl_z}} = 0.$$

Since

$$\frac{\partial}{\partial f_{rl_z}} \begin{bmatrix} f_{fr_z} \\ f_{fl_z} \\ f_{rr_z} \end{bmatrix} = \begin{bmatrix} -1 \\ 1 \\ 1 \end{bmatrix},$$

we have

$$-c_{fr} f_{fr_z} + c_{fl} f_{fl_z} + c_{rr} f_{rr_z} - c_{rl} f_{rl_z} = 0 . \tag{5}$$

$$\begin{bmatrix} m & 0 & 0 & \mu_{fr_x} & \mu_{fl_x} & \mu_{rr_x} & \mu_{rl_x} \\ 0 & m & mb & \mu_{fr_y} & \mu_{fl_y} & \mu_{rr_y} & \mu_{rl_y} \\ 0 & mb & I_{zz}+mb^2 & \ell\mu_{fr_y}-d\mu_{fr_x} & \ell\mu_{fl_y}+d\mu_{fl_x} & -d\mu_{rr_x} & d\mu_{rl_x} \\ 0 & 0 & 0 & -1 & -1 & -1 & -1 \\ 0 & mh & I_{xz}+mbh & -d & d & -d & d \\ -mh & 0 & 0 & \ell & \ell & 0 & 0 \\ 0 & 0 & 0 & -1 & 1 & 1 & -1 \end{bmatrix} \begin{bmatrix} \dot{v}_x \\ \dot{v}_y \\ \dot{r} \\ f_{fr_z} \\ f_{fl_z} \\ f_{rr_z} \\ f_{rl_z} \end{bmatrix} + \begin{bmatrix} -mv_yr-mbr^2 \\ mv_xr \\ mbv_xr \\ 0 \\ mhv_xr \\ mhv_yr+(I_{xz}+mbh)r^2 \\ 0 \end{bmatrix} + \begin{bmatrix} 0 \\ 0 \\ 0 \\ -mg \\ 0 \\ mgb \\ 0 \end{bmatrix} = \begin{bmatrix} 0 \\ 0 \\ 0 \\ 0 \\ 0 \\ 0 \\ 0 \end{bmatrix} \tag{6}$$

This equation, known as compatibility equation, enables the explicit derivation of four reaction forces due the static load distribution, and the longitudinal and lateral load transfer. Note that the compatibility equation introduces four strain parameters which may affect the behavior of the model. How to choose the four strain parameters in an appropriate way, however, goes beyond the scope of this work where the aim has been to expose the mathematical ideas underlying the development of the car model.

Note that by setting $c_{ij} = 1$, $\forall i \in \{f, r\}, j \in \{r, l\}$, the compatibility equation (5) gives us the least squares solution to

$$\mathcal{M}_{22}\lambda = -(\mathcal{M}_{21}\dot{q}_v + \mathcal{C}_2 + \mathcal{G}_2).$$

In this case, the normal forces are given by

$$\begin{aligned} f_{fr_z} =& -\frac{mgb - mh\dot{v}_x + mhv_yr + (I_{xz}+mbh)r^2}{2\ell} \\ &+ \frac{mh\dot{v}_y + (I_{xz}+mbh)\dot{r} + mhv_xr}{d} \\ f_{fl_z} =& -\frac{mgb - mh\dot{v}_x + mhv_yr + (I_{xz}+mbh)r^2}{2\ell} \\ &- \frac{mh\dot{v}_y + (I_{xz}+mbh)\dot{r} + mhv_xr}{d} \\ f_{rr_z} =& -\frac{mga + mh\dot{v}_x - mhv_yr - (I_{xz}+mbh)r^2}{2\ell} \\ &+ \frac{mh\dot{v}_y + (I_{xz}+mbh)\dot{r} + mhv_xr}{d} \\ f_{rl_z} =& -\frac{mga + mh\dot{v}_x - mhv_yr - (I_{xz}+mbh)r^2}{2\ell} \\ &- \frac{mh\dot{v}_y + (I_{xz}+mbh)\dot{r} + mhv_xr}{d} \end{aligned}$$

To sum up, the dynamics of the constrained system is given by Equation (6). For sake of space, we omit the dependence of μ_{ij_x} and μ_{ij_y} from κ_{ij}, β_{ij}, and δ.

III. Model validation on aggressive trajectories

In this section we validate the RigidCar model on an aggressive trajectory with respect to a complex multi-body model. First, we briefly describe the optimal control based strategies used to compute aggressive trajectories of the RigidCar model.

A. Exploration strategy

In order to find a RigidCar trajectory minimizing a suitable distance from a complex model trajectory we pose an optimal control problem defined as

$$\begin{aligned} \min\ & \frac{1}{2}\int_0^T \|x(\tau) - \mathrm{x}_d(\tau)\|_Q^2 + \|u(\tau) - \mathrm{u}_d(\tau)\|_R^2 d\tau \\ & \qquad + \frac{1}{2}\|x(T) - \mathrm{x}_d(T)\|_{P_1}^2 \\ \text{subj. to}\ & \dot{x} = f(x,u) \qquad x(0) = x_0, \end{aligned} \tag{7}$$

where Q, R and P_1 are positive definite weighting matrices, for $z \in \mathbb{R}^n$ and $W \in \mathbb{R}^{n\times n}$ $\|z\|_W^2 = z^T W z$, and $\xi_d := (\mathrm{x}_d(\cdot), \mathrm{u}_d(\cdot))$ is a desired curve. In our model validation set-up the desired state-input curve is (part of) a trajectory of the complex vehicle model, but it is *not* a trajectory of the RigidCar model. In particular, in the numerical computations we acquire the desired curve from a multi-body tool (Adams/Car).

Several techniques are available to solve optimal control problems. We use the PRojection Operator based Newton method for Trajectory Optimization (`PRONTO`) developed in [17]. However, the optimal control problem that we want to solve is an optimization problem in the infinite dimensional space of state-input curves subject to highly nonlinear dynamics. This means that the solution is highly influenced by the desired curve and by the initial trajectory. For this reason, we use an exploration strategy, developed in [14], combining the `PRONTO` algorithm with morphing and continuation ideas. We refer the reader to [14] for a detailed discussion on the exploration strategy.

Note that the exploration strategy guarantees the convergence to a local minimum of the optimal control problem in (7). This is due to the convergence of the `PRONTO` method and by continuity of the optimal control problem with respect to parameters.

B. Numerical computations: ISO lane change maneuver

We compute the RigidCar trajectory for a ISO lane change maneuver. The car model parameters are based on a four-wheeled vehicle of ADAMS/Car tools and are given in [14]. At the beginning the vehicle is at the center of the track, with initial longitudinal speed to $v_{x0} = 100$[km/h] (27.78[m/s]). The vehicle is driven from the initial lane to another parallel lane and back again to the original lane (lane offset 3.5[m]). The comparison between the RigidCar trajectory and the Adams one is shown in Figure 3.

From the numerical computation we observe a good position tracking: the maximum displacement error with respect to the desired position is less than 0.2[m]. In Figure 3b we show the lateral acceleration profile of the RigidCar model versus the Adams vehicle one. We highlight how the

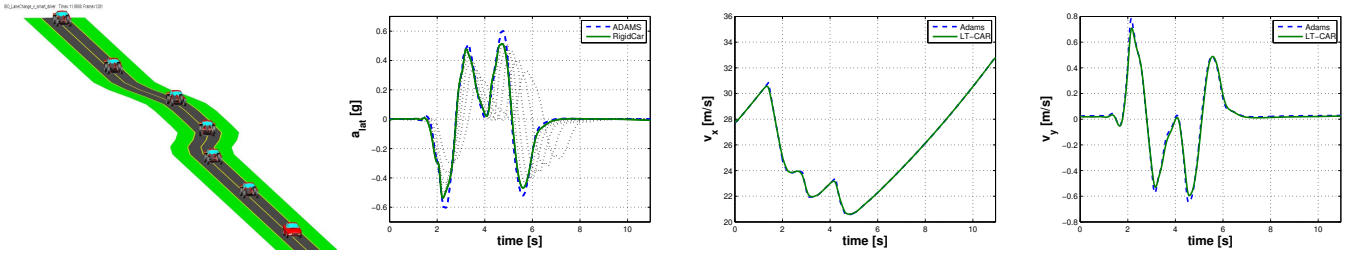

(a) ISO Lane Change maneuver. (b) Lateral acceleration a_{lat}. (c) Longitudinal velocity v_x. (d) Lateral velocity v_y.

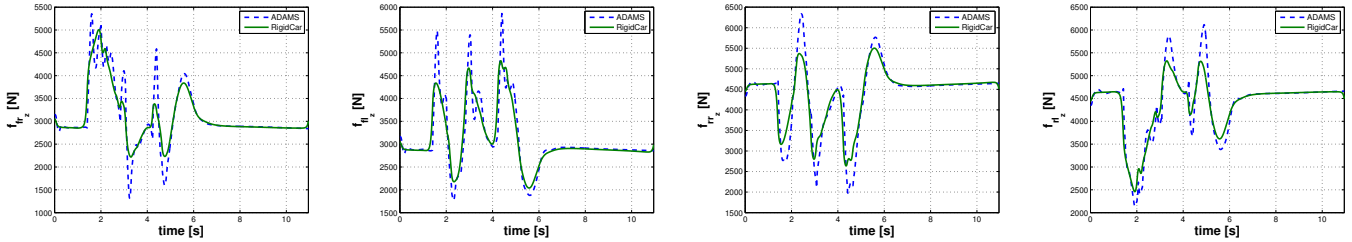

(e) Wheel load f_{fr_z}. (f) Wheel load f_{fl_z}. (g) Wheel load f_{rr_z}. (h) Wheel load f_{rl_z}.

Fig. 3: Aggressive lane change maneuver. In subplot (a) a snapshot of the ISO lane change maneuver is shown. In (b) the optimal RigidCar lateral acceleration (solid line) and the Adams lateral acceleration (dash line) are shown. Temporary optimal RigidCar trajectories are in light dot lines. In (c) and (d) longitudinal and lateral velocity profiles of RigidCar and Adams are compared. In (e)-(f)-(g)-(h) the normal foces f_{ij_z} at the four contact points are shown.

RigidCar trajectory profile continuously morph with a "non-aggressive" acceleration, in light dot line, into the actual trajectory profile with maximum performance, in solid line. However, we observe that Adams model reaches higher values of lateral acceleration than those of the RigidCar model. In particular, the maximum lateral acceleration is, approximately, 0.6[g] for the Adams model, and 0.53[g] for the RigidCar model. In Figure 3c and Figure 3d we show the longitudinal and lateral speed profiles, respectively. We observe that the RigidCar velocity profiles match accurately the Adams ones: the maximum error is less 0.41[m/s] for the longitudinal speed and 0.1[m/s] for the lateral one. Finally, in Figures 3e, 3f, 3g, and 3h, we show that, with the exception for transients due to the suspension model, the RigidCar model predicts the Adams load transfer although the RigidCar has not a suspension model.

IV. Conclusions

In this paper we introduced a novel reduced-order two-track car model that includes tire models, longitudinal and lateral load transfer, without modeling the suspensions. The proposed model is validated by using an exploration strategy based on optimal control techniques. The numerical computations confirm that the model captures the main dynamic features of a full-vehicle model, such as the longitudinal and lateral load transfer, with a low computational effort. The proposed model can be used in handling analysis and controller design, for example in a model predictive control scheme, and, thus, needs further investigations.

References

[1] T. D. Day, "An overview of the HVE vehicle model," in *SAE, paper no. 950308*, 1995, pp. 55–68.

[2] R. Frezza and A. Beghi, "A virtual motorcycle driver for closed-loop simulation," *IEEE Control Systems Magazine*, vol. 5, pp. 62–77, 2006.

[3] W. F. Milliken and D. L. Milliken, *Race car vehicle dynamics*. SAE International, 1995.

[4] T. D. Gillespie, *Fundamentals of Vehicle Dynamics*. SAE, Warrendale, 1992.

[5] R. Rajamani, *Vehicle Dynamics and Control*. Springer, 2006.

[6] H. B. Pacejka, *Tire and Vehicle dynamics*. Butterworth Heinemann, 2002.

[7] M. Villella, "Nonlinear modeling and control of automobiles with dynamic wheel-road friction and wheel torque inputs," Ph.D. dissertation, Georgia Institute of Technology, 2004.

[8] U. Kiencke and L. Nielsen, *Automotive Control Systems for Engine, Driveline, and Vehicle*. Springer Verlag, 2005.

[9] M. Klomp, *Longitudinal Force Distribution and Road Vehicle Handling*. Chalmers University of Technology, 2010.

[10] R. S. Sharp and D. A. Crolla, "Road vehicle suspension system design - a review," *Vehicle System Dynamics*, vol. 16, no. 3, 1987.

[11] A. Rucco, G. Notarstefano, and J. Hauser, "Computing minimum lap-time trajectories for a single-track car with load transfer," in *IEEE Conf. on Decision and Control*, Maui, Hawaii, USA, December 2012.

[12] H. Dugoff, P. Fancher, and L. Segal, "An analysis of tire traction properties and their influence on vehicle dynamic performance," in *SAE, paper no. 700377*, vol. 4, 1970.

[13] C. Canudas de Wit, P. Tsiotras, E. Velenis, M. Basset, and G. Gissinger, "Dynamic friction models for road/tire longitudinal interaction," *Vehicle System Dynamics*, vol. 39, no. 3, 2003.

[14] A. Rucco, G. Notarstefano, and J. Hauser, "Optimal control based dynamics exploration of a rigid car with load transfer," 2011. [Online]. Available: http://arxiv.org/pdf/1112.1530.pdf

[15] ——, "Dynamics exploration of a single-track rigid car model with load transfer," in *IEEE Conf. on Decision and Control*, Atlanta, GA, USA, December 2010.

[16] J. Matheson, *Hyperstatic structures: an introduction to the theory of statically indeterminate structures*. Butterworths, 1971, no. v. 1.

[17] J. Hauser, "A projection operator approach to the optimization of trajectory functionals," in *IFAC World Congress*, Barcelona, 2002.